

PCCP

Accepted Manuscript



This is an *Accepted Manuscript*, which has been through the Royal Society of Chemistry peer review process and has been accepted for publication.

Accepted Manuscripts are published online shortly after acceptance, before technical editing, formatting and proof reading. Using this free service, authors can make their results available to the community, in citable form, before we publish the edited article. We will replace this *Accepted Manuscript* with the edited and formatted *Advance Article* as soon as it is available.

You can find more information about *Accepted Manuscripts* in the [Information for Authors](#).

Please note that technical editing may introduce minor changes to the text and/or graphics, which may alter content. The journal's standard [Terms & Conditions](#) and the [Ethical guidelines](#) still apply. In no event shall the Royal Society of Chemistry be held responsible for any errors or omissions in this *Accepted Manuscript* or any consequences arising from the use of any information it contains.

Transport Diffusivity of Propane and Propylene inside SWNTs from Equilibrium Molecular Dynamics Simulations

Hongjun Liu

Chemical Sciences Division, Oak Ridge National Laboratory, Oak Ridge, Tennessee 37831

To whom correspondence should be addressed. E-mail: liuh1@ornl.gov.

ABSTRACT

The gas transport of two model gases (propane and propylene) inside the single-wall nanotubes (SWNTs) of various diameters was systematically investigated using the molecular dynamics (MD) simulations. The thermodynamic factor can be obtained directly from equilibrium MD simulations following the newly-minted method proposed by Schnell *et al.* (*Chem. Phys. Lett.* 2011, 504, 199-201). This process eliminates the need to implement the tedious and challenging Monte Carlo simulations for the adsorption isotherm, from which the thermodynamic factor is usually extracted. The satisfactory agreement between simulation and the literature is found for self-diffusivity, corrected diffusivity and transport diffusivity, as well as the thermodynamic factor. The ideal selectivity for propane/propylene mixture through SWNT membranes could be optimized through adjusting the concentration gradient. This method can be readily extended to the binary and multiple-component systems.

Keywords: Transport diffusivity, equilibrium molecular dynamics, gas transport in SWNT, paraffin/olefin separation.

1. Introduction

A wide variety of porous membrane materials such as zeolite, metal-organic framework, covalent organic framework, polymeric, *etc.* can be used for separation application.¹⁻⁵ An efficient membrane requires high selectivity and permeability. Yet, the performance of membrane is usually limited by the trade-off of selectivity and permeability.⁶ Searching for new materials to overcome the upper bound is a dominant theme in membrane science. Carbon nanotube (CNT) is especially promising to overcome the Robeson bound due to its effective adsorption capacity and extremely high diffusivity.⁷⁻¹² CNTs have shown a great potential as a stable and effective adsorbent for hydrogen storage and for separation of various mixtures.¹³⁻¹⁵ Diffusion inside CNTs can be orders of magnitude faster than that in other porous material of comparable size. This can be explained by smoothness of energy landscape inside CNTs.⁹

Understanding gas transport through porous membrane is essential for effective separation application. Among several distinct diffusion properties, transport diffusivity defined by the net gas flux over a pressure/concentration gradient is of greatest interest.^{8, 16, 17} Transport diffusivity is defined by the Fick's law, also known as Fickian diffusivity or collective diffusivity. Transport diffusivity is strongly influenced by the adsorption equilibrium and not easily connected with simple molecular interpretation. It is necessary to adopt a more fundamental concept to provide the molecule-level understanding for macroscopic transport. In the Maxwell-Stefan formulation of irreversible thermodynamics,¹⁸⁻²⁰ transport diffusivity can be related to a multiple of corrected diffusivity (D_0) and thermodynamic factor (Γ). The term RT/D_0 can be interpreted as the drag coefficient between gas molecules and the pore wall. This formula provides one of the mostly used ways to compute transport diffusivity in molecular simulations, where both quantities are accessible. Specifically, corrected diffusivity is estimated from the trajectories of equilibrium MD simulation and thermodynamic factor is computed by differentiation of the adsorption isotherm obtained in grand canonical Monte Carlo (GCMC) simulation. However, GCMC simulation of dense phases at room temperature is rather challenging since the insertion and deletion of molecules is infamously inefficient at crowded environment.

Recently, Vlugt group has proposed a novel method to directly compute thermodynamic factor from small-scale density fluctuation in equilibrium MD simulations.²¹ This method has been validated in homogenous system of Lennard-Jones fluid,²² molecular fluid mixture,²³ and in heterogeneous system of zeolite.²⁴ In this work, we extend this efficient method to investigate the SWNTs of various sizes and show the method works well in this important class of system. The paper is organized as follows. In Section 2, we present the methodology and explain how to obtain corrected diffusivity and thermodynamic factor from equilibrium MD, therefore transport diffusivity. The simulation details are also provided. In Section 3, we show the results and discuss what we have learned from simulations. In Section 4, we summarize our conclusions.

2. Methods

Molecular dynamics simulation was applied to investigate the gas transport in SWNTs. Various quantities can be used to describe the kinetics of gas through the framework. The most straightforward one is self-diffusivity D_s , which describes the random motion of adsorbate molecules at thermodynamic equilibrium. It can be estimated using Einstein relation through the mean squared displacement of tagged molecule:

$$D_s = \frac{1}{2N} \lim_{t \rightarrow \infty} \frac{1}{t} \left\langle \sum_{i=1}^N (\mathbf{r}_i(t) - \mathbf{r}_i(0))^2 \right\rangle \quad (1)$$

, where N is the number of gas molecules in the system and $\mathbf{r}_i(t)$ is the position vector of particle i at time t . The angle bracket denotes the ensemble average. Note that the prefactor of 2 is for the axial diffusion of gas molecules in nanotube. Yet, the property that is more relevant to depict the mass transport across a framework membrane of certain length is the transport diffusivity D_t , also known as Fickian diffusivity. D_t can be related to the flux as a prefactor to the concentration gradient by the Fick's law:

$$\mathbf{J} = -D_t(c) \frac{dc}{dz} \quad (2)$$

Transport diffusivity cannot be readily calculated from the simulation, instead that two related quantities (corrected diffusivity D_0 and thermodynamic factor Γ) are estimated. Based on the Maxwell-Stefan formulation of non-equilibrium thermodynamics, the following relationship is given:

$$D_t = D_0 \left(\frac{\partial \ln f}{\partial \ln c} \right)_T = D_0 \Gamma \quad (3)$$

, where f is the fugacity in thermodynamic equilibrium with the concentration of c . Thermodynamic factor is the concentration derivative of fugacity describing the deviation from the ideal behavior. The corrected diffusivity or Maxwell-Stefan diffusivity D_0 can be readily calculated from MD simulation through the following equation:

$$D_0 = \frac{1}{2N} \lim_{t \rightarrow \infty} \frac{1}{t} \left\langle \left(\sum_{i=1}^N (\mathbf{r}_i(t) - \mathbf{r}_i(0)) \right)^2 \right\rangle \quad (4)$$

Note that D_0 is related to the MSD of the center of mass of all adsorbate molecules and is a reflection of facility for the collective motion of adsorbed molecules. Equation (4) only holds for unary system, and the related expressions for binary system can be found elsewhere.^{16, 19} For the thermodynamic factor, one usually need differentiate the adsorption isotherms obtained from the grand canonical MC simulations. Recently, Vlught group proposed an efficient method to calculate thermodynamics of a small non-periodic system in a large periodic reservoir. Small embedded system can exchange particle and energy with the reservoir, similar to a system in the grand canonical ensemble. One can compute the thermodynamic factor as the density fluctuation directly from equilibrium MD simulations:

$$\frac{1}{\Gamma} = \frac{\langle N^2 \rangle - \langle N \rangle^2}{\langle N \rangle} \quad (5)$$

A series of small systems were sampled in the canonical ensemble trajectory to plot $1/\Gamma$ vs. $1/L$. The thermodynamic limit can be recovered from

$$\frac{1}{\Gamma} = C \frac{1}{L} + \frac{1}{\Gamma_{\infty}} \quad (6)$$

In the heterogeneous system, the shape of the small systems is essential for proper sampling. One should choose the small sampling shape commensurate with the underlying framework structure. For instance, the zeolite system can be properly sampled by the small systems consisting of at least one crystallographic unit cell in all directions.²⁴ As for the SWNT, the small sampling region varies only by unit cell along the axial direction, while keeps the cross-section included in the radial direction. Once the transport diffusivity as a function of concentration or loading known, one can obtain the steady-state flux of gas across of a framework of length L :

$$J = \frac{1}{L} \int_{c_{out}}^{c_{in}} D_t(c) dc \quad (7)$$

where c_{in} and c_{out} are concentrations of upstream and downstream, respectively. The ideal selectivity of binary mixture is defined as the ratio of flux of component i over flux of component j under the one-component condition.

$$S_{ij}^{ideal} = \frac{J_i^{neat}}{J_j^{neat}} \quad (8)$$

The SWNT framework is rigid and keeps fixed during the simulation course, since the tube flexibility is only important for lighter molecules in the limit of zero loading.²⁵ Carbon atoms of SWNT are represented as graphite carbon with Lennard-Jones parameter ($\sigma = 3.4 \text{ \AA}$ and $\epsilon = 0.05564 \text{ kcal mol}^{-1}$). Gas molecules are modelled by the united-atom model, and each CH_x unit is represented by a Lennard-Jones bead. The force field parameters follow the TraPPE-UA.²⁶ CH_3 bead has σ of 3.75 \AA and ϵ of $0.19475 \text{ kcal mol}^{-1}$, CH bead has σ of 3.73 \AA and ϵ of $0.0934 \text{ kcal mol}^{-1}$, and CH_2 bead has σ of 3.675 \AA and ϵ of $0.16891 \text{ kcal mol}^{-1}$. All bonds are rigid with the single bond length of 1.54 \AA and double bond length of 1.33 \AA . Both angles are flexible. The angle of propane is with an equilibrium θ of 114° and k_θ of $124.2 \text{ kcal mol}^{-1}$, and the angle of propylene with an equilibrium θ of 119.7° and k_θ of $139.94 \text{ kcal mol}^{-1}$. The cross terms are evaluated by the Lorentz-Berthelot mixing rule. The potential

cutoff is 12 Å and with the tail correction.

Molecular dynamics simulations were carried out in the NVT ensemble. All simulations were simulated with LAMMPS package.²⁷ PBC was applied only along the axial direction of SWNTs. Nose-Hoover thermostat was used to keep the system temperature at 300 K. The zigzag-type (n,0) SWNT of 198.8 Å was studied at different gas loadings. The length of SWNT is 100 Å. The diameters of SWNT of (10,0), (12,0), (14,0), (16,0) and (20,0) are 7.8 Å, 9.4 Å, 11.0 Å, 12.5 Å and 15.7 Å, respectively. The SHAKE algorithm was used to constrain the bonds.²⁸ The timestep is 1 fs and trajectory was dumped every 2 ps. The 100-ns trajectory was used to extract the structural and dynamic properties.

3. Results and discussions

Mean squared displacement can reflect the diffusion mechanism. $MSD \propto t^2$ represent the ballistic diffusion, while $MSD \propto t$ denotes the Fickian diffusion, which is the intrinsic diffusion mechanism of bulk fluid phase. For diffusivity measurement, one should go to the diffusive region to fit the slope; otherwise, the serious error is expected. Figure 1 presents the logarithmic plot of MSD of propane molecules inside different SWNTs at loading of 1 molecule/nm at 300 K. The loading is related to pressure by the adsorption isotherm of gas molecules. The representative lines of ballistic and Fickian diffusion are also included. The double-log plot makes the recognition of diffusion mechanism easier. Inside larger-size SWNTs (20,0) and (16,0) MSDs reveal the transition from the ballistic to Fickian around a few tens of picoseconds, while for smaller size SWNTs, the transition trend is the ballistic to Fickian to super-diffusion to Fickian. The ballistic diffusion sometimes is missing in MSD plot due to a big timestep or a low sample frequency on trajectory. The diffusion inside SWNT can be explained by the cooperation of the small confinement and periodic surface. The small confinement comparable to the molecular diameter suppresses the radial motion of gas molecules, resulting in frequent collisions along the axial direction in the intermediate time. This might explain the super-

diffusion observed in smaller size SWNTs.

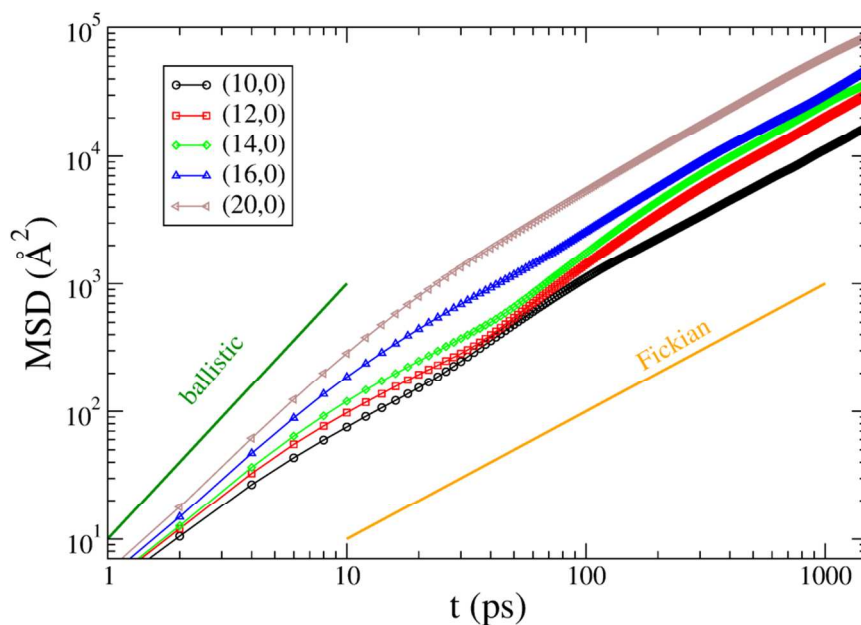


Figure 1. Mean squared displacement of C_3H_8 inside SWNTs at loading of 1 molecule/nm. Diffusivity is estimated through fitting between 200 ps and 2 ns.

Figure 2 depicts the propane orientation inside SWNTs. CH_2 bead prefers to stay away from carbon atoms in the framework than CH_3 does, since CH_3 group interacts more favorably with carbon atoms of framework. If there is enough space for gas molecules to orientate themselves freely (that is certainly the case for larger size SWNTs), CH_2 stays closer to the axis of SWNT, while CH_3 locates next to the wall of SWNT. Yet, the space is so restricted inside (10,0) SWNT with a diameter of 7.8 Å that propane molecule has to orientate its molecular axis normal to the axis of SWNT to accommodate itself (the angle between the axis of nanotube and molecular axis, α , peaks at 90°). The molecular axis of propane is defined as the vector normal to the CH_3 - CH_3 passing CH_2 bead.

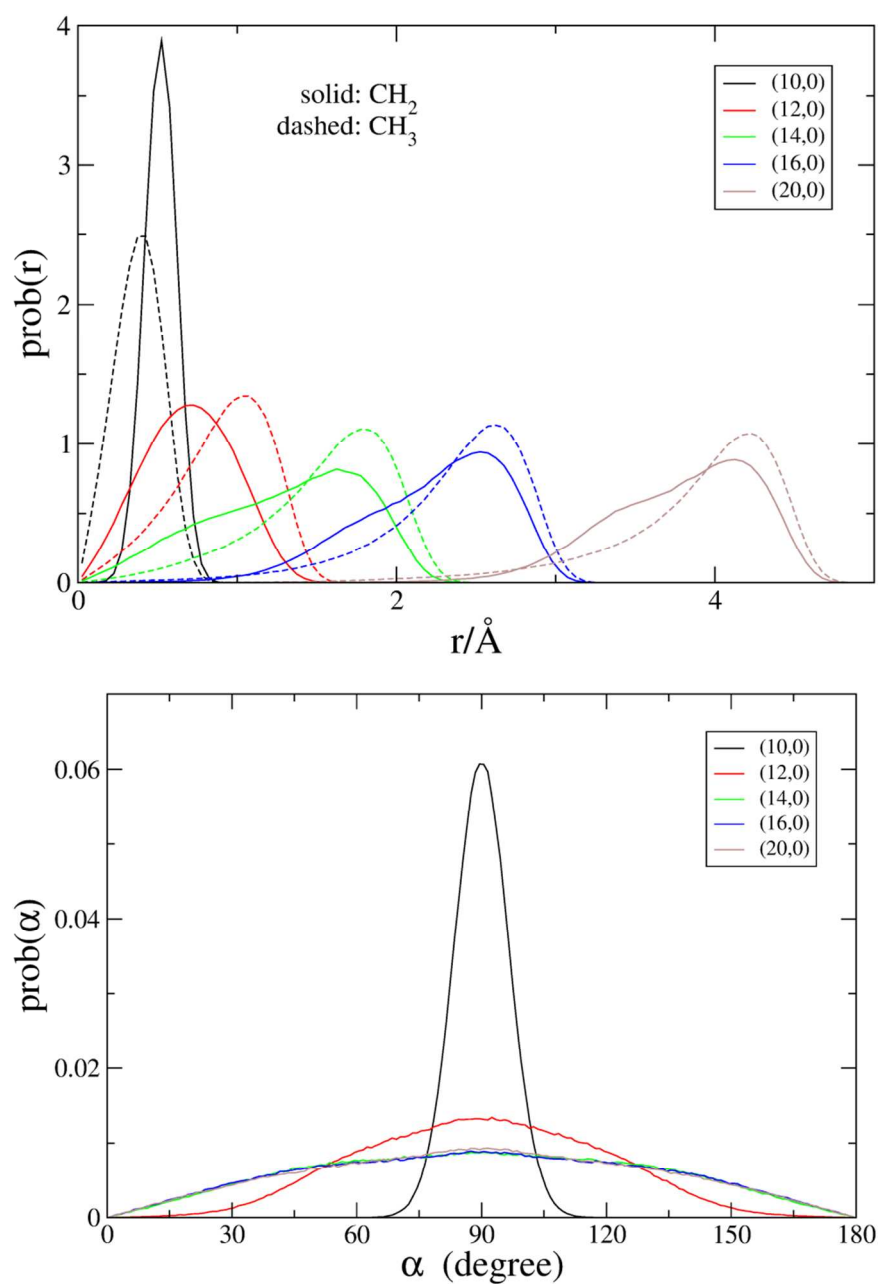


Figure 2. C_3H_8 conformation in SWNTs with loading of 1 molecule/nm. The distance from the axis of SWNTs is r and the angle between the axis of nanotube and molecular axis is α .

The mean squared displacement of propylene inside (16,0) SWNT at different loadings is presented in logarithm scale in Figure 3. The behavior is similar to what the confinement effect has been shown in Figure 1. One can clearly see the diffusion behavior of propylene follows the ballistic at short time, while the Fickian at longer time when the loading does not exceed 1 molecule/nm. Further

increasing loading, there is no ballistic region observed due to the overcrowded molecular environment and longer timestep. The transition of Fickian-super-diffusion-Fickian is evident for higher loadings.

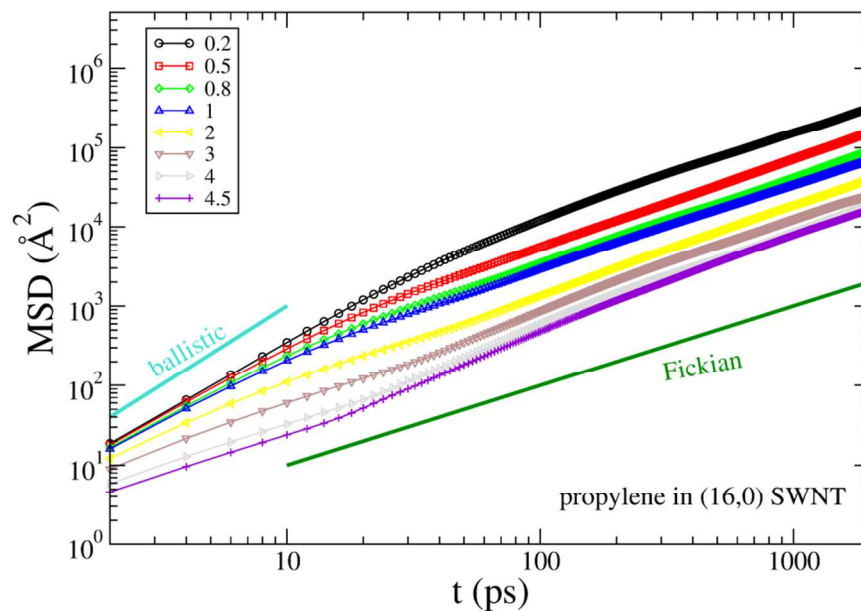


Figure 3. Mean squared displacement of C_3H_6 in (16,0) SWNT at different loadings.

From the long-time diffusive region, the gas mobility can be examined by the self-diffusivity and corrected diffusivity. Figure 4 shows the resulting diffusivity data of propane inside SWNTs as a function of loading. In the limit of infinite dilution, $D_s = D_0 = D_t$. Since the tube flexibility is essential for properly describing molecule diffusion in the limit of zero loading,²⁵ we are not in position to discuss the self-diffusivity trend under such conditions. Increasing loading leads to a reduced self-diffusivity. The range of D_s covers almost three orders of magnitude as loading varies. Loading effect on self-diffusivity is more pronounced at low loadings than at higher loadings. D_s becomes less sensitive to loading as loading increases. Generally, self-diffusivity increases with the size of SWNT especially at intermediate and high loadings, which was also observed in the methane simulation¹⁶ and CO_2 simulation.¹⁷ Gas molecules are well known to diffuse much faster inside SWNTs of a few molecular diameters than in other materials of comparable sizes.⁹ The self-diffusivities of propane

inside SWNTs are about two orders of magnitude larger than that in 1-D channel of zeolite and the higher self-diffusivities can be explained by the much smoother energy landscape in SWNTs than that in zeolite.⁹ The corrected diffusivities of propane in SWNTs are almost independent of loading, which was also demonstrated for CH₄ inside the silica micropores (diameter less than 2 nm).²⁹ The values of D_0 range from 0.02 to 0.04 cm²/s as the loading varies. This is in stark contrast with the self-diffusivity, which decreases by about three orders of magnitude. The insensitivity of corrected diffusivity is typical of the weakly confinement scenario, where adsorbate molecules are weakly confined inside the adsorbent framework.³⁰

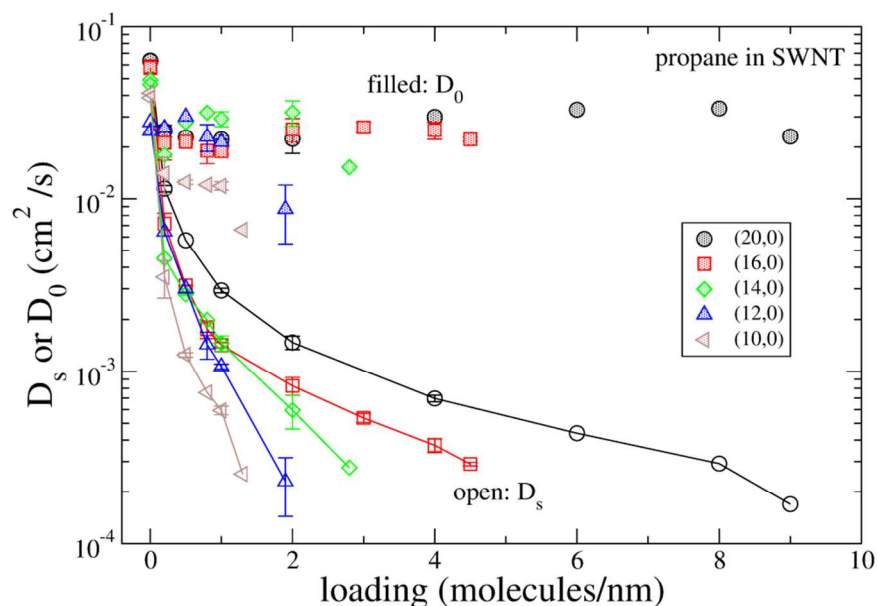


Figure 4. Self and corrected diffusivities of C₃H₈ inside SWNTs. The lines are just guide to the eye.

The error bars are from multiple independent runs.

To obtain the information on transport diffusivity, one need come up with a way to estimate the thermodynamic factor. Instead of using the conventional MC method to trace the adsorption isotherm, we applied the recently proposed method to obtain Γ directly from equilibrium MD simulations.

Thermodynamic factor depends on system size and can be computed from fluctuations at the

nanoscale. In our case, the small systems are embedded in a NVT ensemble reservoir. The results for thermodynamic factor for one model system (14,0) are presented in Figure 5 as a function of inverse length of small sampling system. Note that the size of small system is required to be significantly smaller than that of reservoir. Through the linear regression, thermodynamic factor in the thermodynamic limit is obtained. Loading effect on thermodynamic factors of propane and propylene inside SWNTs is examined in Figure 6. As expected, at low loading, thermodynamic factor approaches unity. For smaller SWNTs, thermodynamic factor is monotonic increasing function of loading. Γ of (20,0) SWNT decreases first then increases with loading. The difference in Γ between propane and propylene is vanishingly small at low loadings, while at high loadings the thermodynamic factor of propane is always larger than that of propylene.

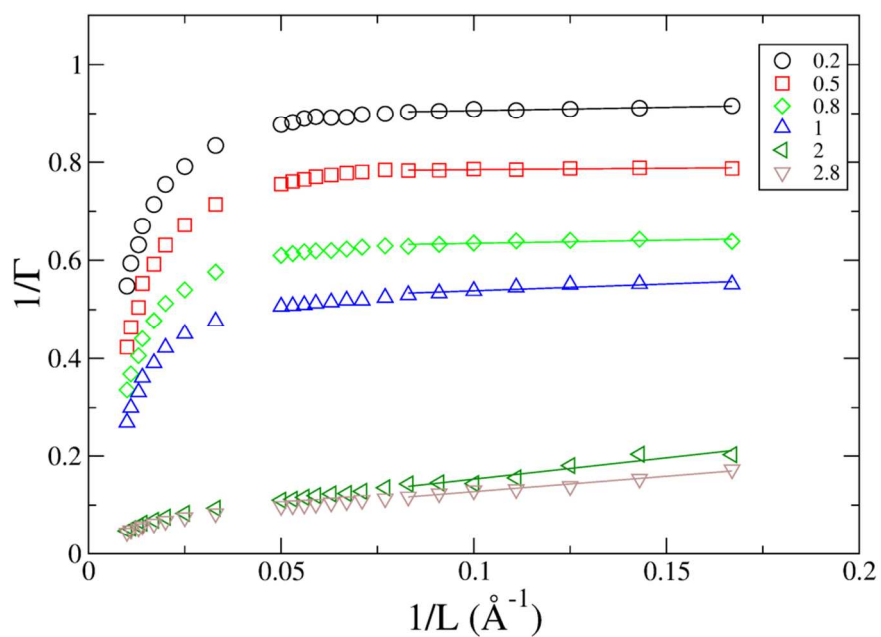


Figure 5. Inverse thermodynamic factor (symbols) as a function of inverse sampling system length in (14,0) SWNT at different loadings ranging from 0.2 molecule/nm to 2.8 molecule/nm. Γ_∞ is obtained from the linear regression (denoted by lines).

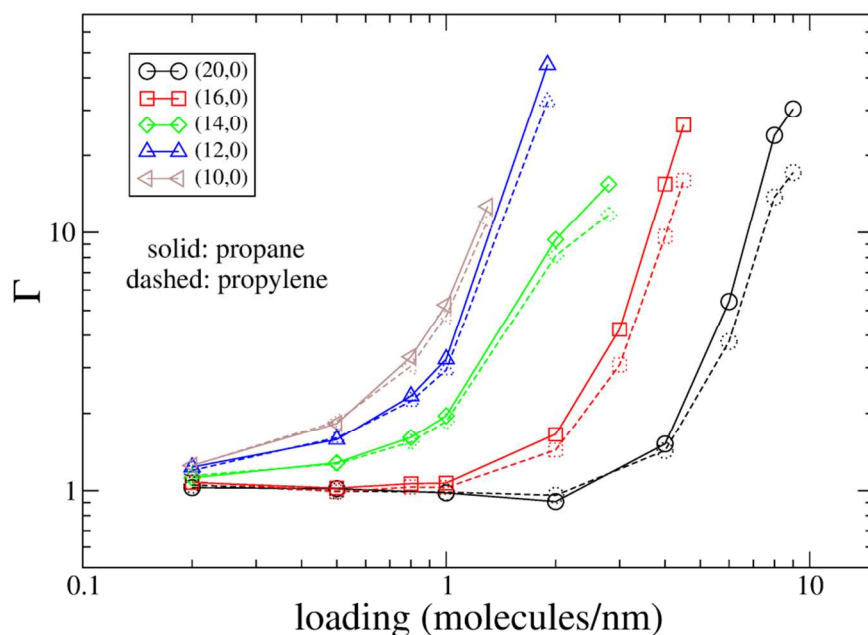


Figure 6. Thermodynamic factor of C_3H_8 and C_3H_6 as a function of loading in SWNTs. The error is smaller than the size of symbols.

All diffusivity data (D_s , D_0 and D_t) of propane and propylene inside (16,0) SWNT is presented in Figure 7. One can see the relative magnitude of three diffusivities. D_s is the smallest one, and decreases markedly with loading; while D_t , being the largest one, increases with loading; D_0 is practically independent of loading, locating in between. The D_t difference between inside SWNTs ($0.01 \text{ cm}^2/\text{s} - 1 \text{ cm}^2/\text{s}$) and in zeolites ($10^{-13} - 10^{-9} \text{ cm}^2/\text{s}$) is much larger than the difference in D_s .³¹ Moreover, transport diffusivity inside SWNTs is comparable to the bulk diffusivity of neat gas (without restraining walls).¹⁶ Loading dependence of D_t is dominantly dictated by the thermodynamic factor due to the insensitivity of D_0 . The moderate decrease of D_t at low loadings is due to the slight decrease of Γ , while the rapid increase at high loadings is a direct consequence of the similar increase in Γ . The initial decreases in D_t followed by an increase was also observed in other gases inside SWNTs.^{8, 32} In this relatively large-size SWNT, transport diffusivity of propane is larger than that of propylene at high loading, and slightly less at low loadings. In contrast, propylene always diffuses faster than propane in

terms of self and corrected diffusivities over the whole loading range.

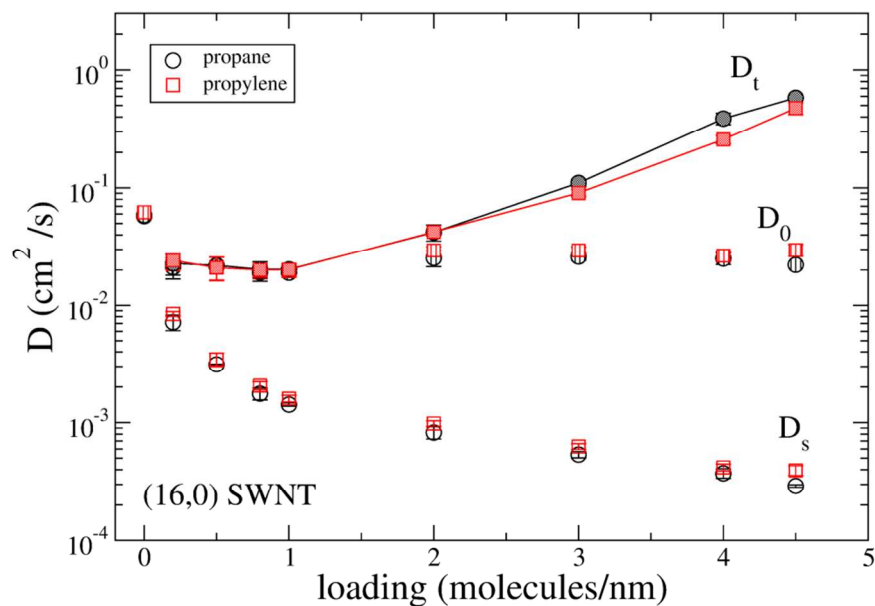


Figure 7. Diffusivities of C_3H_8 and C_3H_6 in (16,0) SWNT. Solid filled: D_t , vertical filled: D_0 and open: D_s .

Loading dependence of transport diffusivities of propane and propylene inside SWNTs is shown in Figure 8. The recent study proposed that the detailed picture on gas diffusion inside SWNTs involves surface diffusion and Knudsen diffusion.¹⁷ In the former, most gas molecules adsorb on the wall of SWNTs and diffuse downstream along the tubular structure as shown in Figure 2(a). Note that the LJ diameter of C is 3.4 Å and that of CH₃ bead is around 3.7 Å. In the latter, several molecules can travel cross the nanotube diameter and make collision with the framework. At low loadings, gas molecules are effectively trapped near the nanotube wall, and only a few can escape; thereby surface diffusion dominates. As a result, gas molecule diffuses faster in the larger-size SWNTs. At high loadings and much more gas molecules can enter SWNT; extra layers of gas tubular structure could form. Now gas molecule could probably flow in its own layer, instead of interrupt with other layers. The transport diffusivity is generally inversely proportional to the size of SWNTs. This observation applies to both propane and propylene. The similar behavior was also found in CO₂ simulation with

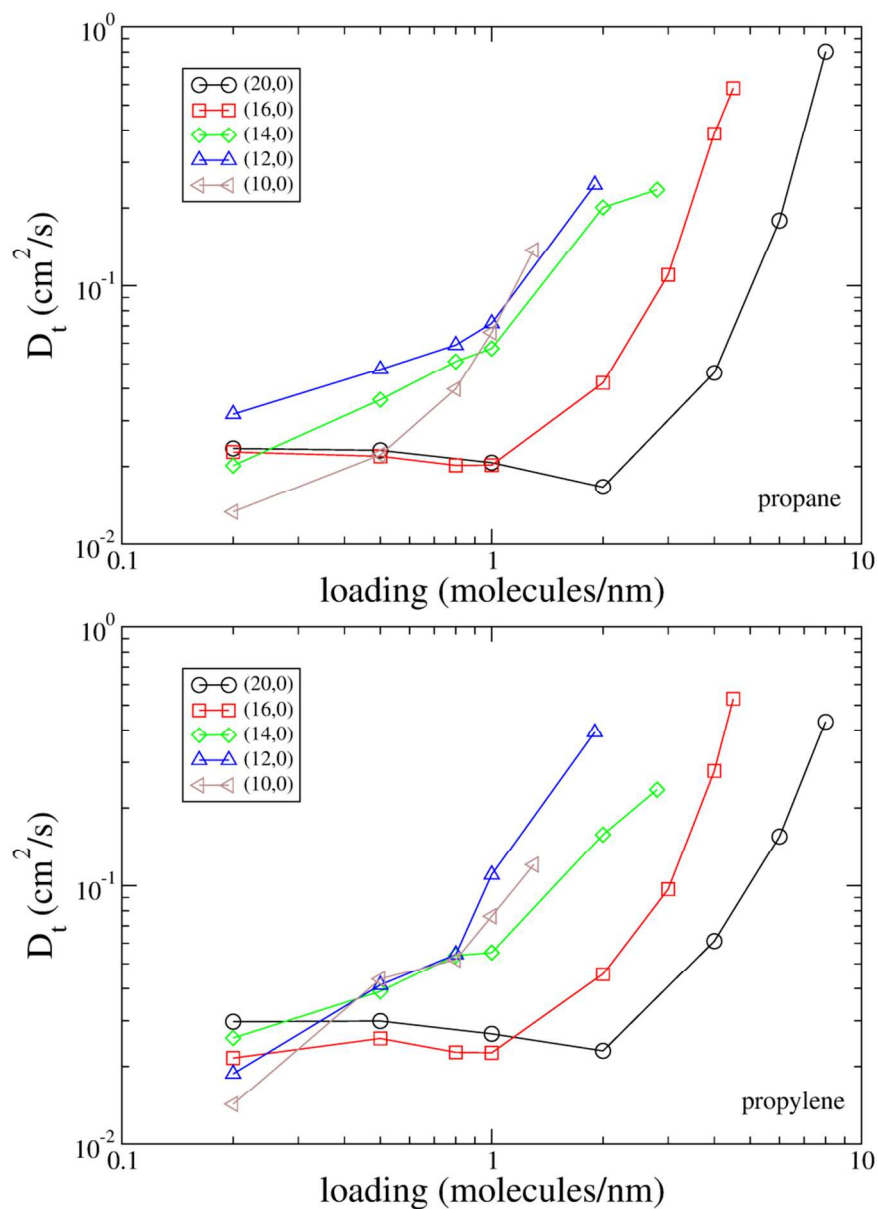
SWNTs.¹⁷

Figure 8. Loading dependence of transport diffusivities of C_3H_8 (upper panel) and C_3H_6 (lower panel) inside SWNTs.

We can estimate the flux of gas molecules through a hypothetical membrane of a length of 10 nm by assuming the zero loading is a good approximation for the downstream pressure accessed in the experiment. The ideal selectivity for the propane/propylene mixture through this imaginary membrane can be computed through the ratio of fluxes of pure components. The resulting S^{ideal} is depicted in

Figure 9. Generally, the ideal selectivity is rather small, in the range of 0.7 – 1.7. In the larger-size SWNTs, propane is favored at high loadings, while propylene is favored at low loadings. In (12,0) SWNT, the opposite trend is observed. In the smallest (10,0) SWNT, propylene is always favored. The selectivity could be adjusted through fine-tuning of pressure/loading gradient, as shown by Arora and Sandler.⁸

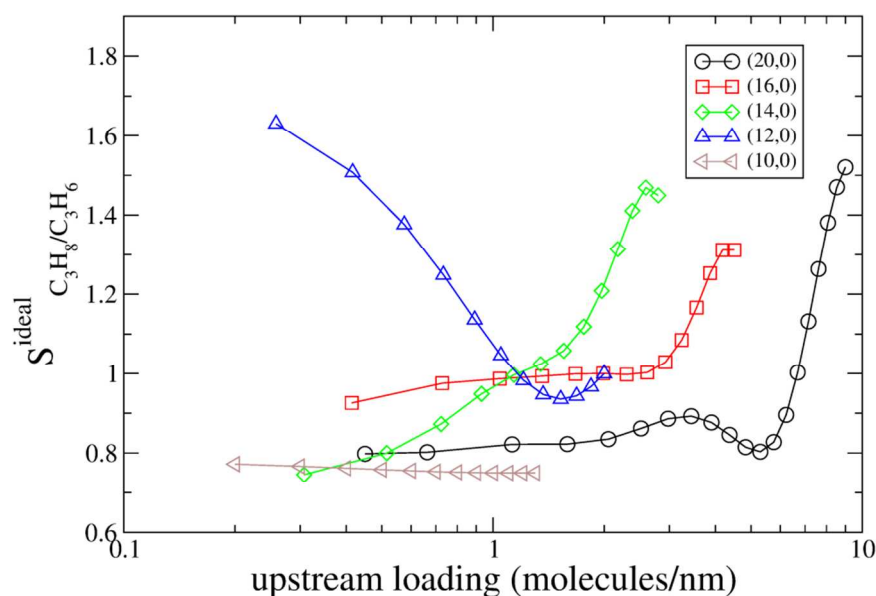


Figure 9. Ideal selectivity of C_3H_8/C_3H_6 in a 10nm-length SWNT membrane at zero downstream loading.

4. Conclusions

We have systematically investigated gas transport of propane and propylene inside SWNTs of various diameters using the molecular dynamics simulations. With help of the newly-minted method, we can compute the thermodynamic factor directly from equilibrium MD simulations. This process eliminates the tedious MC simulations for the adsorption isotherm, from which the thermodynamic factor is usually extracted. The agreement between this work and the literature is satisfactorily well for self-diffusivity, corrected diffusivity and transport diffusivity, as well as the thermodynamic factor.¹⁶

Self-diffusivity decreases with loading and loading effect is more pronounced at low loadings than at higher loadings. Corrected diffusivity is almost independent of loading, indicating the weak confinement of gas molecules in SWNT adsorbent framework. Transport diffusivity is dominated by the thermodynamic factor increases with loading in small-size SWNTs, and decreases first then increases with loading in large-size SWNTs. The surface diffusion appears to be dominant. Transport diffusivity inside SWNTs is comparable to diffusivity of unconfined gas and several orders of magnitude greater than those in other porous materials. The ideal selectivity for propane/propylene mixture through SWNT membranes is rather small. The better selectivity could be achieved through fine-tuning of pressure gradient. This efficient method can be readily extended to the binary or multiple-component systems.

Acknowledgement

We thank Drs. De-en Jiang and Sheng Dai. This work was supported by the Division of Chemical Sciences, Geosciences, and Biosciences, Office of Basic Energy Sciences, U.S. Department of Energy. This research used resources of the National Energy Research Scientific Computing Center (NERSC), which is supported by the Office of Science of the U.S. Department of Energy under Contract No. DE-AC02-05CH11231.

References

1. Czaja, A. U.; Trukhan, N.; Muller, U., Industrial applications of metal-organic frameworks. *Chem Soc Rev* 2009, 38, 1284-1293.
2. Li, J. R.; Kuppler, R. J.; Zhou, H. C., Selective gas adsorption and separation in metal-organic frameworks. *Chem Soc Rev* 2009, 38, 1477-1504.
3. Davis, M. E., Ordered porous materials for emerging applications. *Nature* 2002, 417, 813-821.

4. Feng, X.; Ding, X. S.; Jiang, D. L., Covalent organic frameworks. *Chem Soc Rev* 2012, 41, 6010-6022.
5. Bernardo, P.; Drioli, E.; Golemme, G., Membrane Gas Separation: A Review/State of the Art. *Ind Eng Chem Res* 2009, 48, 4638-4663.
6. Robeson, L. M., Correlation of Separation Factor Versus Permeability for Polymeric Membranes. *J Membrane Sci* 1991, 62, 165-185.
7. Arora, G.; Sandler, S. I., Air separation by single wall carbon nanotubes: Thermodynamics and adsorptive selectivity. *J Chem Phys* 2005, 123.
8. Arora, G.; Sandler, S. I., Air separation by single wall carbon nanotubes: Mass transport and kinetic selectivity. *J Chem Phys* 2006, 124.
9. Skoulidas, A. I.; Ackerman, D. M.; Johnson, J. K.; Sholl, D. S., Rapid transport of gases in carbon nanotubes. *Phys Rev Lett* 2002, 89.
10. Chen, H. B.; Sholl, D. S., Rapid diffusion of CH₄/H₂ mixtures in single-walk carbon nanotubes. *J Am Chem Soc* 2004, 126, 7778-7779.
11. Sokhan, V. P.; Nicholson, D.; Quirke, N., Transport properties of nitrogen in single walled carbon nanotubes. *J Chem Phys* 2004, 120, 3855-3863.
12. Chen, H. B.; Sholl, D. S., Predictions of selectivity and flux for CH₄/H₂ separations using single walled carbon nanotubes as membranes. *J Membrane Sci* 2006, 269, 152-160.
13. Arab, M.; Picaud, F.; Devel, M.; Ramseyer, C.; Girardet, C., Molecular selectivity due to adsorption properties in nanotubes. *Phys Rev B* 2004, 69.
14. Jiang, J. W.; Sandler, S. I., Nitrogen and oxygen mixture adsorption on carbon nanotube bundles from molecular simulation. *Langmuir* 2004, 20, 10910-10918.
15. Challa, S. R.; Sholl, D. S.; Johnson, J. K., Adsorption and separation of hydrogen isotopes in carbon nanotubes: Multicomponent grand canonical Monte Carlo simulations. *J Chem Phys* 2002, 116, 814-824.
16. Krishna, R.; van Baten, J. M., Describing binary mixture diffusion in carbon nanotubes with the Maxwell-Stefan equations. An investigation using molecular dynamics simulations. *Ind Eng Chem Res* 2006, 45, 2084-2093.
17. Skoulidas, A. I.; Sholl, D. S.; Johnson, J. K., Adsorption and diffusion of carbon dioxide and nitrogen through single-walled carbon nanotube membranes. *J Chem Phys* 2006, 124.
18. Krishna, R., Problems and Pitfalls in the Use of the Fick Formulation for Intraparticle Diffusion. *Chem Eng Sci* 1993, 48, 845-861.
19. Krishna, R., Describing the Diffusion of Guest Molecules Inside Porous Structures. *J Phys Chem C* 2009, 113, 19756-19781.
20. Krishna, R.; Wesselingh, J. A., Review article number 50 - The Maxwell-Stefan approach to mass transfer. *Chem Eng Sci* 1997, 52, 861-911.
21. Schnell, S. K.; Vlugt, T. J. H.; Simon, J. M.; Bedeaux, D.; Kjelstrup, S., Thermodynamics of a small system in a μT reservoir. *Chem Phys Lett* 2011, 504, 199-201.
22. Schnell, S. K.; Vlugt, T. J. H.; Simon, J. M.; Bedeaux, D.; Kjelstrup, S., Thermodynamics of small systems embedded in a reservoir: a detailed analysis of finite size effects. *Mol Phys* 2012, 110, 1069-1079.
23. Liu, X.; Schnell, S. K.; Simon, J. M.; Bedeaux, D.; Kjelstrup, S.; Bardow, A.; Vlugt, T. J. H., Fick Diffusion Coefficients of Liquid Mixtures Directly Obtained From Equilibrium Molecular Dynamics. *J Phys Chem B* 2011, 115, 12921-12929.
24. Schnell, S. K.; Liu, X.; Simon, J. M.; Bardow, A.; Bedeaux, D.; Vlugt, T. J. H.; Kjelstrup, S., Calculating Thermodynamic Properties from Fluctuations at Small Scales. *J Phys Chem B* 2011, 115, 10911-10918.
25. Jakobtorweihen, S.; Lowe, C. P.; Keil, F. J.; Smit, B., Diffusion of chain molecules and mixtures

- in carbon nanotubes: The effect of host lattice flexibility and theory of diffusion in the Knudsen regime. *J Chem Phys* 2007, 127.
26. Potoff, J. J.; Siepmann, J. I., Vapor-liquid equilibria of mixtures containing alkanes, carbon dioxide, and nitrogen. *Aiche J* 2001, 47, 1676-1682.
27. Plimpton, S., Fast Parallel Algorithms for Short-Range Molecular-Dynamics. *J Comput Phys* 1995, 117, 1-19.
28. Ryckaert, J. P.; Ciccotti, G.; Berendsen, H. J. C., Numerical-Integration of Cartesian Equations of Motion of a System with Constraints - Molecular-Dynamics of N-Alkanes. *J Comput Phys* 1977, 23, 327-341.
29. Bhatia, S. K.; Nicholson, D., Adsorption and Diffusion of Methane in Silica Nanopores: A Comparison of Single-Site and Five-Site Models. *J Phys Chem C* 2012, 116, 2344-2355.
30. Skoulidas, A. I.; Sholl, D. S.; Krishna, R., Correlation effects in diffusion of CH₄/CF₄ mixtures in MFI zeolite. A study linking MD simulations with the Maxwell-Stefan formulation. *Langmuir* 2003, 19, 7977-7988.
31. Pan, Y. C.; Li, T.; Lestari, G.; Lai, Z. P., Effective separation of propylene/propane binary mixtures by ZIF-8 membranes. *J Membrane Sci* 2012, 390, 93-98.
32. Ackerman, D. M.; Skoulidas, A. I.; Sholl, D. S.; Johnson, J. K., Diffusivities of Ar and Ne in carbon nanotubes. *Mol Simulat* 2003, 29, 677-684.